






## Structural, Thermal and Electrical Properties of Modified Borate-Based Glass

Aya A. Alhar<sup>1\*</sup>, Firas J. Hmood<sup>1</sup>, Ahmed O. Al-Roubaiy<sup>2</sup>

<sup>1</sup> Department of Ceramic Engineering and Building Materials, College of Materials Engineering, University of Babylon, Babylon 51002, Iraq

<sup>2</sup> Department of Metallurgy, College of Materials Engineering, University of Babylon, Babylon 51002, Iraq

Corresponding Author Email: [aya.ahmed.math98@student.uobabylon.edu.iq](mailto:aya.ahmed.math98@student.uobabylon.edu.iq)

Copyright: ©2024 The authors. This article is published by IIETA and is licensed under the CC BY 4.0 license (<http://creativecommons.org/licenses/by/4.0/>).

<https://doi.org/10.18280/rcma.340410>

### ABSTRACT

**Received:** 19 April 2024

**Revised:** 27 May 2024

**Accepted:** 15 June 2024

**Available online:** 27 August 2024

#### Keywords:

*borate glass, borosilicate glass, glass transition temperature, kinetic window*

Borate glasses are of interest for many electronic applications like electronic packages and in vacuum systems as sealing glass. The aim of this work is to study the effect of  $Pb_2O_3$  and  $SiO_2$  additives on the structural and characteristics of borate glass. Binary borate glass of  $BaO.B_2O_3$  was synthesized by melt-quenching technique. The additives were introduced to the glass by substitution with  $BaO$  and  $B_2O_3$ . Two batches of six recipes were prepared. All the synthesized glasses were transparent. The glass transition temperature ( $T_g$ ) has varied according to the chemical composition. Recipe G3 exhibits the lowest  $T_g$  around  $440^\circ C$ , while G2 and G4 show high thermal stability. Coexisting of  $Pb^{2+}$  and  $Si^{4+}$  led to high dielectric constant for glass G5 and G6.

## 1. INTRODUCTION

Generally, glass containing boron serves in many technical applications for instance electrical [1] and medical [2] applications. Introducing rare-earth elements to glass helps taking glass to another level of technical fields. Barium borate glass is industrially important. It has found its applications in optics like glass fibers, electronic packages and radiation protection as barium is a heavy metal [3-5]. Besides, it has many attractive thermal and chemical features that makes it a good candidate to serve as sealing glass [6].

Barium oxide is colorless with a density of  $5.72 \text{ g/cm}^3$  [7]. It is considered an intermediate oxide because it has the ability to be glass former or modifier. Not all the compositions in  $BaO-B_2O_3$  forms glass; however, compositions of high ratio of  $B_2O_3$ ,  $BaO$  can form easily glass. Namely, the composition  $BaO.2B_2O_3$  is congruently melting compound and melts at  $900^\circ C$ .

Like fluids, glass can be used as sealing material for many reasons. For instance, it has good resistance to environmental conditions and ability to bind different materials (components) like glass-glass, ceramic-glass, metal-glass or mixing of them [8-10]. Among the preceding joints glass-to-metal seals are very important in the construction of vacuum tubes, electric discharge tubes, incandescent light bulbs, glass-encapsulated semiconductor diodes reed switches, glass windows in metal cases, and metal or ceramic-packages of electronic components and many others [11].

In addition, it can be widely used in range of optical and electrical fields because it has a high dielectric constant ( $\epsilon_r$ ) like in large electrical energy storage capacity and in capacitors and other parts where a high permittivity is preferred [12].

Two methods can be followed to develop the properties of this binary glass represented by doping [13-16] and heat treatment [17]. Both of the two strategies induced microstructural changes in boron network. The variation of properties as a result of introducing cations in the network of glass formers rely on the cations radii as well as the field strength of cations. For instance, cations that generate non-bridging oxygen decreases the glass transition temperature ( $T_g$ ) and vice-versa. Cations like  $Al^{3+}$  which make complex coordination tend to increase  $T_g$  [18]. On the other hand, heat treatments of glass induce essential changes in glass network. They enhance formation crystalline phases in glass matrix. The new phases have different compositions and hence different properties than that of the parent glass.

The first route was followed in this work. In which lead oxide was replaced by barium oxide. It is widely used in protection from radiation as it has large density ( $11.34 \text{ g/cm}^3$ ) which allows it to absorb radiations of different wavelengths. Lead can also improve the processing features of glass by increasing the thermal stability and widening the working range of glass [19]. Careful engineering of glass composition, microstructure, viscosity, and reactivity enables reliable joining of glasses with metals through stake, match, and butt seal configurations [20].

### 1.1 Glass design

In this study, binary and ternary borate glass were synthesized to develop glass with low processing temperatures based on the phase diagrams illustrated in Figure 1.

Two glass batches were designed. Each batch involved three recipes. The first batch is formed based on a binary glass system of  $BaO-B_2O_3$ , spatially  $BaB_2O_4$ . This glass

characterized by high refractive index and low light dispersion [5]. The selected stoichiometric composition is 30BaO·70B<sub>2</sub>O<sub>3</sub> as illustrated in Figure 1(a). This composition melts at 910°C [21].

In the ternary system, silica was also added to borate glass to form ternary system of BaO·SiO<sub>2</sub>·B<sub>2</sub>O<sub>3</sub> of eutectic point at a mole ratio of 3:3:2, respectively. It has good ability to form glass at relatively low processing temperatures at around 1000°C [21]. Lowering the processing temperatures is of demand as it saves energy and decrease volatilization of light doping elements like boron.

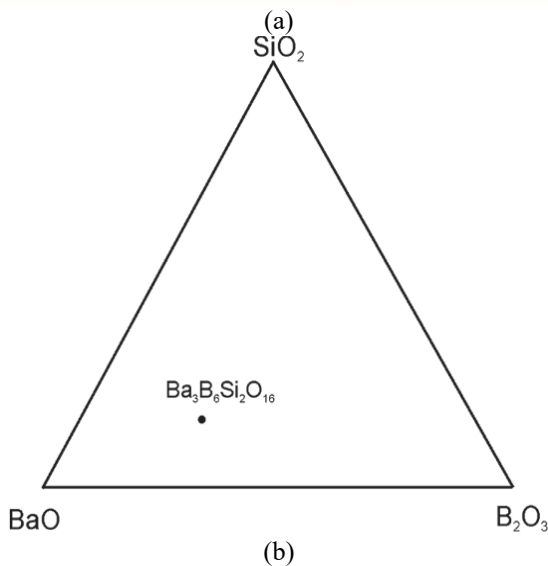
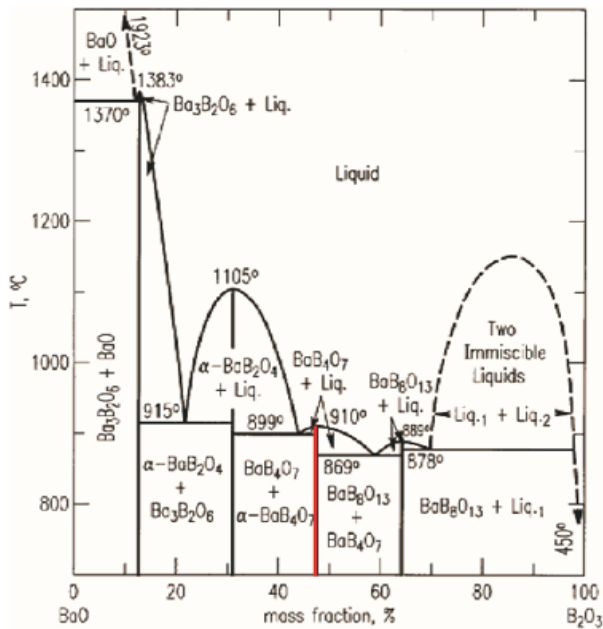


**Figure 1.** (a) Binary phase diagram of BaO·B<sub>2</sub>O<sub>3</sub> [15];  
(b) Ternary phase diagram of BaO·B<sub>2</sub>O<sub>3</sub>·SiO<sub>2</sub>

Lead oxide (Pb<sub>2</sub>O<sub>3</sub>) was introduced by substitution with BaO and B<sub>2</sub>O<sub>3</sub>, respectively, in the first batch. Whereas, it substituted by BaO only in the second batch, as seen in Table 1, to lower the melting temperature as low as possible. The anticipated application for this glass is metal sealing which necessitate low thermal expansion coefficient to minimize the thermal stresses in glass. Laser assisted sealing is an interesting technique of sealing because it is eco-friendly technique and exposes possibility to control the required energy of sealing [22].

The aim of this study is to synthesize binary and ternary borate glass with modifying the chemical composition. This will make the glass more useful for other technological applications. In addition to investigate the effects of structural changes on the thermal and electrical characteristics of borate glass. To achieve this purpose, the strategy of doping was implemented to have lead oxide in the glass compositions.

**Table 1.** Chemical composition of glass

Glass Recipes	Components (mol%)			
	BaO	B <sub>2</sub> O <sub>3</sub>	SiO <sub>2</sub>	Pb <sub>2</sub> O <sub>3</sub>
Batch I	G1	30	70	----
	G2	20	70	10
	G3	30	60	10
Batch II	G4	37.5	37.5	25
	G5	27.5	37.5	10
	G6	10	37.5	25

## 2. Experiments

### 2.1 Glass powder synthesis

The starting materials of this study were barium carbonate 99.5% (BaCO<sub>3</sub>), boric acid 99.0% (H<sub>3</sub>BO<sub>3</sub>), lead oxide (Pb<sub>2</sub>O<sub>3</sub>) and silica (SiO<sub>2</sub>) (Central drug house (P) Ltd., India). 10 g of each glass recipe were prepared according to the mole ratios stated in Table 1. The powders were mixed together using a planetary mill for 45 min in dry condition. Alumina crucibles were used to melt the constituents at temperatures between 950°C to 1100°C depending on the chemical composition. The glass melt was kept at these temperatures for 20 min to lower the volatilization of boron and other elements. The melts were then quenched in water and finally milled and sieved through 200 μm sieve.

### 2.2 Characterizations

#### 2.2.1 Structural characteristics

The structure of yield glass was investigated using x-ray diffraction means. An x-ray diffractometer (type: XRD 6000, manufactured by Shimadzu, Japan) was implanted to carry on this investigation. In which copper- $\alpha$  was utilized as a radiation source with 40 kV and 30 mA with a scanning speed of 5°/min. Nickel filter was used in the travel way of x-ray before striking the sample, which is moving in a circular motion. When the incident beam diffracts according to Bragg's law, diffraction occurs, as shown in Eq. (1) [14].

$$n \lambda = 2d \sin \theta \quad (1)$$

On the other hand, the active groups of the glass structure were identified by Fourier transform infrared (FTIR) spectroscopy (Shimadzu1800, Japan) over the range from 4000 to 400 cm<sup>-1</sup>. Samples of glass powder were mixed with KBr (10%) and pressed at 10 Tons/cm<sup>2</sup>.

#### 2.2.2 Thermal characteristics

Simultaneous thermal analysis (STA 449C, Netzsch, Germany) was used to determine the characteristics temperatures. 50 mg of each glass was heated up to 900°C in an alumina crucible at normal dried air atmosphere at a heating rates of 10 K/min.

### 2.2.3 Dielectric properties

Hioki LCR Impedance Analyzer (IM 3570, Japan) was used to measure the dielectric constant. The samples were cylindrical ( $\phi 5 \times 7L$ ) mm. silver paste ( $20 \Omega m$ ) was applied on the samples ends to make them electrically conductive. The dielectric constant ( $\epsilon_r$ ) was calculated mathematically according to the following equation  $(t \times C_p)/A$  at 1 MHz. Where  $t$ : thickness of the ceramic sample (mm),  $C_p$ : capacity of glass (pF),  $t$ : sample thickness (mm). The electrical resistivity was calculated according to the ratio  $(\rho = R_p \times A/l)$ . Where  $A$  is the cross-sectional area and  $l$  represents the length of sample [23].

### 2.2.4 Thermal characteristics

Simultaneous thermal analysis (STA 449C, Netzsch, Germany) was used to determine the characteristic temperatures. 50 mg of each glass powder was heated up to  $900^\circ C$  in an alumina crucible at normal dried atmosphere at a heating rates of 10 K/min. The targeted information are the characteristic temperatures.

The thermal expansion coefficient (TEC) of the yield glass was measured using a dilatometer (model L75 platinum series /Linseis /Germany) as shown in Figure 2. In a non-isotherm heating. The heating rate was 10 K/min and the glass samples were heated upto  $400^\circ C$ . The testing samples were prepared by casting glass in a steel mold (see Figure 2) and subsequently heat treated at  $500^\circ C$  for 2h. Finally, they were cut out to cylinders of ( $5\phi \times 20 L$  mm) using a diamond cutter.

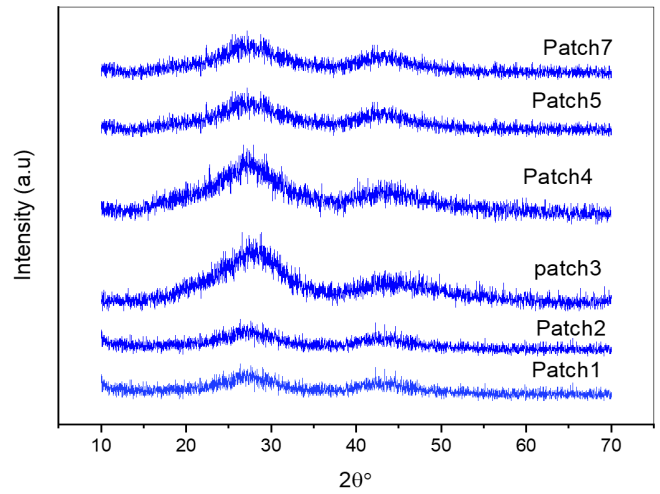


**Figure 2.** Casting of glass sample for dilatometer test: (a) and (b): The mold two sides; (c) Glass cast for dilatometer

## 3. RESULTS AND DISCUSSION

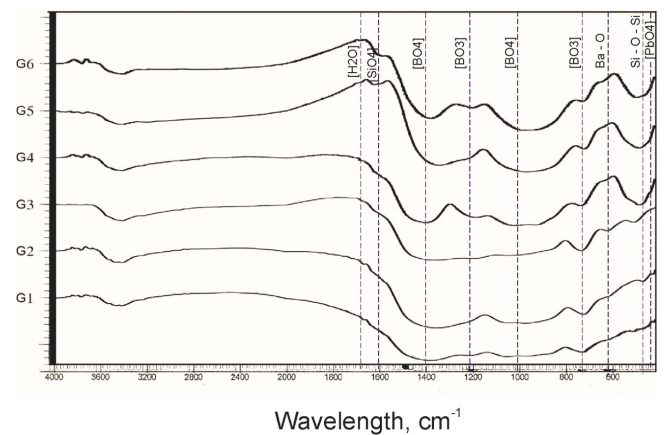
### 3.1 Glass structure

Figure 3 shows the X-ray diffraction of the synthesized glass. The resulting patterns indicate that all the prepared glasses have amorphous structure, where no sharp peaks appeared. In addition, absence of secondary phases reveals that  $Pb_2O_3$  and  $SiO_2$  dissolved well in the glass networks.



**Figure 3.** X-Ray diffraction patterns of the synthesized glass batches

Borate glass appears in their network two building units of boron ( $BO_3$  and  $BO_4$ ) which they possessing totally different connecting environments. Likewise, the network of silica borate glass consists of three distinct building units. Two of them belongs to boron groups and the third returns to silicon group ( $SiO_4$ ) [24, 25]. The spectra of FTIR transmittance are considered an effective means to identify the above connected groups via their (stretching or/and bending) vibrational responses to IR. The structure of borate glass, denoted as (G1), have changed with the substitution of Ba for Pb and Si as seen in Figure 4. Obviously, the network of recipes G1 – G3 exhibits B-O vibrations of triangle group [ $BO_3$ ] at transmittance bands of  $750$  and  $1200 \text{ cm}^{-1}$  [26, 27]. The Band at  $1000$  and  $1400 \text{ cm}^{-1}$  return to four folded boron units [ $BO_4$ ]. The bond Ba-O has a trace at  $600 \text{ cm}^{-1}$  [28].



**Figure 4.** Active bonds in the structure of the synthesized glasses

Barium and lead oxides can be assigned in glass network either as glass formers or as modifiers. Substitution of Ba with Pb in G1 glass has changed connections of the building units. The area under the band at  $750 \text{ cm}^{-1}$  increases from G1-G3 which refer to an increase in content of  $BO_3$  building units. This, however, indicates that PbO has functioned as modifier in the glass. In the same context,  $BO_4$  content at  $1400 \text{ cm}^{-1}$  decreased as a consequence of PbO effect. The transmittance band at the region  $415 - 470 \text{ cm}^{-1}$  may refer to formation  $PbO_4$  tetrahedra, which have the ability to enter the network of boron as Pb-O-B [29-31].

Glass recipes (G4-G6) show vibrational characteristics of SiO<sub>4</sub> at 470 cm<sup>-1</sup> [32] as denoted in Figure 4 next to BO<sub>3</sub> and BO<sub>4</sub>. The transmittance band at 1000 cm<sup>-1</sup> refers to BO<sub>4</sub> and SiO<sub>4</sub> groups as there is an overlap at this position [27, 33]. The bands of FTIR spectra for samples G5 and G6 exhibits gradually increase in the content of BO<sub>4</sub> content with increasing the substitution of barium for lead. The band at wavelength 1600 cm<sup>-1</sup> may belong to the stretching of the bond Si-O-Si [34, 35]. The band observed at a wavenumber 1620 cm<sup>-1</sup> is owing to the H<sub>2</sub>O [29].

### 3.2 Density and Molar volume

Barium and lead are the heaviest elements in the designed glasses. Accordingly, the density of the resulting glasses varied. Recipe G1 shows the highest density of about 4.6092 g/cm<sup>3</sup>. Replacing of barium and boron by lead decreases the density as indicated in Table 2.

**Table 2.** Density and molar volume of the prepared glasses

Glass Recipes	Density, g/cm <sup>3</sup>	Molar Volume, cm <sup>3</sup> /mol
G1	4.6092	21
Batch I		
G2	4.4130	23
G3	4.4224	25
G4	4.1165	24
Batch II		
G5	4.2860	25
G6	4.5122	27

The density of batch II gradually increased up to 4.5122 g/cm<sup>3</sup> for G6. Because of increasing the content of lead on expense of barium content. The atomic weight of Ba is 137.327 and that of lead is 207.2 [36].

Table 2 shows that the molar volume, which represents the volume of material that occupied one mole, of the prepared glasses has changed differently in the two batches. The first batch shows no trend in changing of molar volume. On the other hand, it increases gradually from glass G4 to G6. It is well-known that the molar volume influenced by the atomic radii. The radii of the constituents: Ba: 253 pm, B: 87 pm, Si: 111 pm, Pb: 154 pm. [36]. An increase of non-bridging oxygen (NBOs) in glass network increases V<sub>m</sub>. It is noticed that the difference of V<sub>m</sub> in G1 and G6 is big. This belongs to increase the BO<sub>3</sub> units accompanied by NBOs.

### 3.3 Thermal characterization

Figure 5 illustrates the DTA traces of all the glass recipes. The behavior of the six recipes was varied according to the chemical composition. Table 3 sums up the important temperatures. Generally, the glass transition temperature of glasses is above 500°C but recipe G3 where its T<sub>g</sub> has determined to around 440°C.

**Table 3.** Characteristics features of the prepared glass

Glass Recipes	T <sub>m</sub> , °C	T <sub>g</sub> , °C	T <sub>x</sub> , °C	ΔT(T <sub>p</sub> -T <sub>g</sub> ), °C
G1	910	595	807	212
Batch I				
G2	875	547	843	296
G3	875	440	560	120
G4	1000	625	---	---
Batch II				
G5	850	506	725	219
G6	850	605	850	245

Figure 5 shows also that not all the samples were thermally stable. Recipes G1-G6, except G4, show exothermic peaks

which indicates that those glasses thermally unstable [28]. The difference between T<sub>g</sub> and T<sub>p</sub> reflects the thermal stability of glass [37]. The largest difference, the more stable glass. DTA trace of recipe G4 exhibits no clear exothermic peak which may refer to a strong glass network, while recipe G2 has a kinetic window of 295°C. This belongs to the high content of bridging oxygen (BOs) as a result of BO<sub>4</sub> and PbO<sub>4</sub> (see Figure 4).

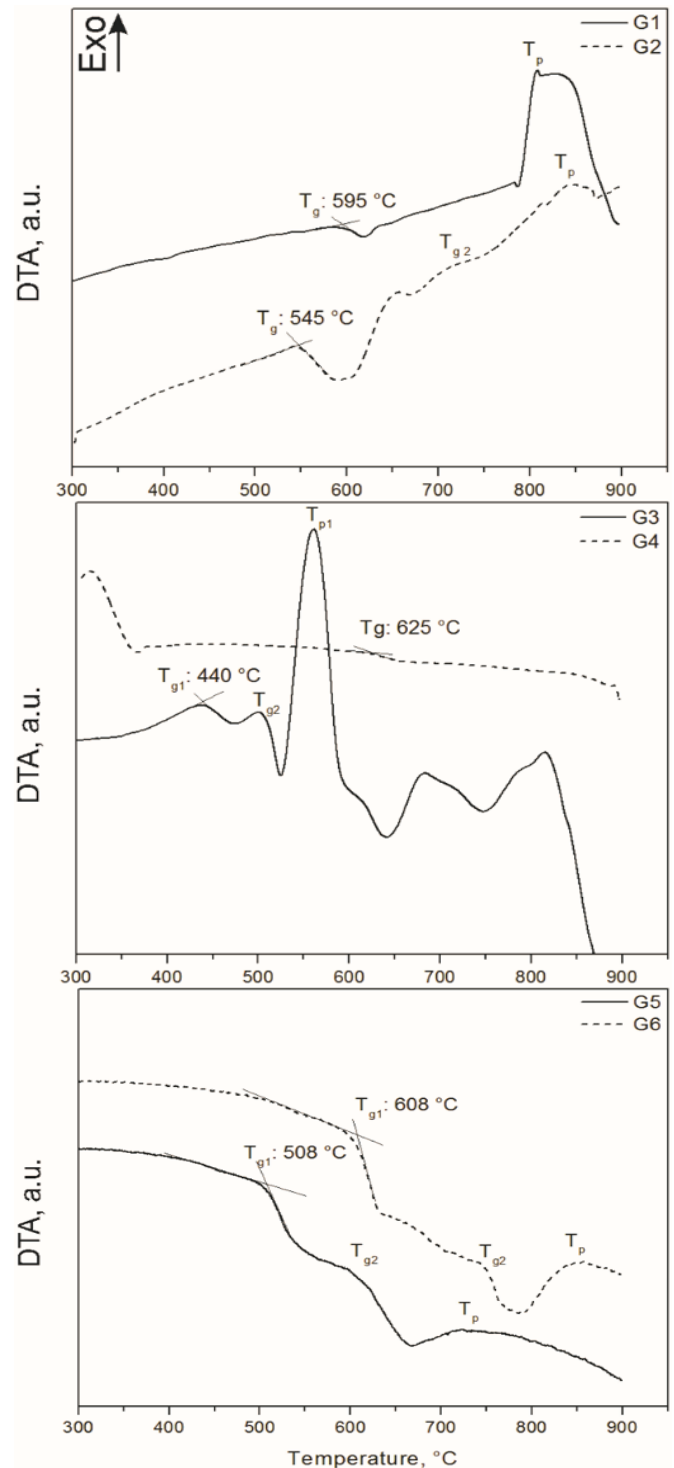


**Figure 5.** Characteristics temperatures of the six recipes

The thermal stability of glass ensures a long working range without challenges of crystallization. The addition of oxide modifiers results in network discontinuity sites, which reduce network cohesiveness and cause the stability of the glass network to be temperature-dependent. The thermal stability of

glasses expressed as  $\Delta T$  reveals that G3 is more prone to crystallize in comparison to G2 which comes with the highest thermal stability. This indicates that lead has worked as glass former in G2 causing an increase in BOs. Whereas in G3 has worked as modifier led to form NBOs resulted in weakening of glass network. Although the change of molar volume is not that big, it might give an indication that PbO acted as modifier in all glasses but G2. G4 has no PbO in its composition. This will, however, produce crystalline phase from the parent glass. The product is called glass-ceramic. The devitrification must be controlled to avoid compromising chemical durability. The resulting properties of glass-ceramics are influenced by the composition of remaining glass in addition to the generated crystalline phases [38].

### 3.4 Thermal expansion coefficient (TEC)

TEC of the synthesized glass was calculated in the range 35-400°C. Figure 6 exhibits TEC of the synthesized glass. The results of recipes G1 and G4 were comparable to the literature. Where recipe G1 ( $BaO \cdot B_2O_3$ ) is between 9.3 and 9.8 ppm  $K^{-1}$  [39] and that of G4 ( $BaO \cdot B_2O_3 \cdot SiO_4$ ) is about 11.29 ppm  $K^{-1}$  [40]. It is obvious that TEC increases for batch I while it decreases for batch II. Generally, the addition of PbO has no that big influence on TEC of the original composition of borate glass. G2 recipe shows a value of 9.3 ppm  $K^{-1}$ . The next lower value belongs G5 recipe of around 9.98 ppm  $K^{-1}$ .

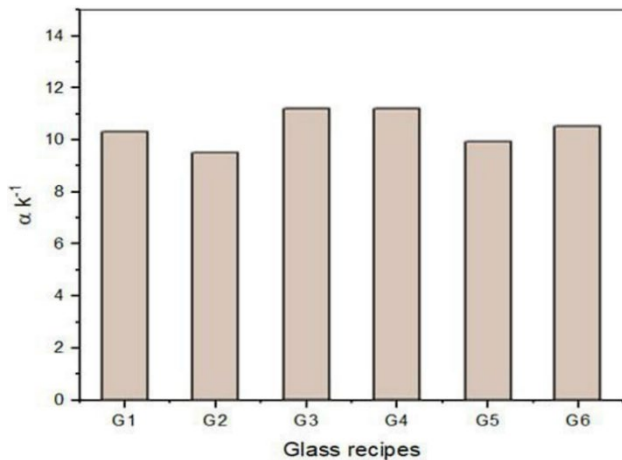


**Figure 6.** Variation of thermal expansion coefficient according to the chemical composition of the yield glass

Figure 4 illustrates that G2 and G5 recipes have higher concentration of bridging oxygen i.e. the building blocks, which belong to the conversion of  $[BO_3]$  to  $[BO_4]$ . While the rest recipes exhibited TEC larger than 10 ppm  $K^{-1}$ . Bobkova reported that alkaline cations in binary borate glass have similar effect as alkalis. In which TEC decreased linearly up to 30-32% mol and then fail to follow the increased content of alkaline (PbO) [41]. This non-linearity tendency is noticeable when two or more alkalines co-exist in glass network.

The experiments have shown that large concentration of PbO generates high concentration of NBO in glass network as supported by the results of Figure 4. It must be referred that the CTE is bond strength dependent of a solid. Introducing PbO on excess of BaO reduces the average bond strength of glass due to the weak bond strength of Pb-O (109 kJ/mol) compared to that of Ba-O (138 kJ/mol) and B-O (498 kJ/mol) [42]. Therefore, the coordination of boron in addition to the net field strength of glass network has affect the thermal

expansion coefficient of the synthesized glass.

### 3.5 Electrical properties

The relative dielectric constant ( $\epsilon_r$ ) of the prepared glasses has varied according to the chemical constituents. Recipe G5 exhibited the highest value of ( $\epsilon_r$ ) of around 2, while recipes G2 has showed the lowest value of about 1.35 (see Figure 7(a)). The structural changes of the glasses have influenced on the ( $\epsilon_r$ ) of the yield glass. Increasing the BOs increase the dielectric constant. As revealed from Figure 4 that the majority of the network units are tetrahedra which means high content of bridging connections and this increases the dielectric constant.

Figure 7(b) exhibits the electrical resistivity of the prepared glasses. It is known that the electrical conductivity in glass counts on the mobility of alkali oxides not on the bivalent oxides [43]. As the prepared glasses are free of alkalis, the resistivity of glasses depends on the concentration of BOs in the glass network. G2 shows the highest electrical resistivity of around 150 M $\Omega$ cm. Moreover, recipe G4 shows  $\rho$  of around 130 M $\Omega$ cm. Introducing of PbO into the network of G4 has contributed in lowering  $\rho$  as well, which diminished the strength of glass network.

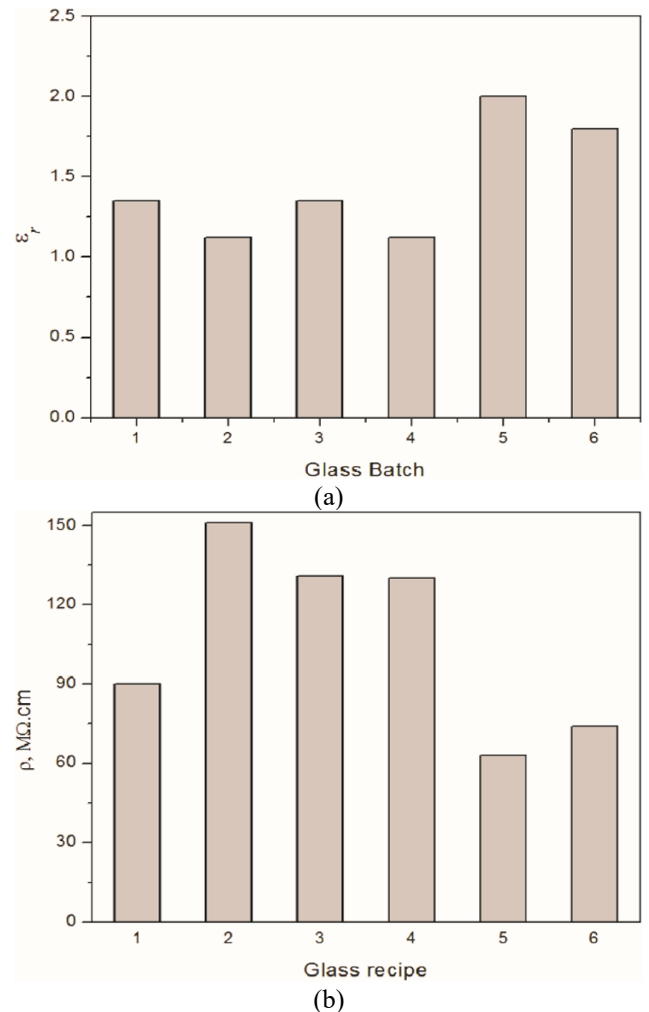


**Figure 7.** Dielectric constant of the prepared borate glass at 1 kHz

Glass with dielectric constant lower than 10 is desirable for many electronic applications. Dielectric constant of glass depends on the ions polarizability, porosity, and concentration

of bridging oxygen in glass structure. Heavy elements like Pb and Ba are considered polarizable ions and glass contains such element characterizes with high dielectric constant [44]. Although the synthesized glasses contain Pb and Ba cations, the resulting dielectric constant is low. This may be related with the concentration of BOs. Boron as glassformer forms open glass network and such condition decreased the dielectric constant. Moreover, boron and silicon cations have less tendency toward polarization. Another reason belongs to the small trapped air bubbles in the synthesized glass samples which in turn lower  $\epsilon_r$ .

The study so far shows promising findings of glass for sealing applications. Insertion other elements in the glass to improve the optical properties will make the glass composition suitable to the advanced sealing technologies like those implement lasers as power sources. Generally, the findings are linked well to the objectives of study and they opened eyes to new glass technologies such as developing sealing methods of glass-metal joints.

#### 4. CONCLUSIONS

The outcomes of study have shown that introducing Pb and Si to barium borate glass has changed its structural and subsequently its thermal characteristics. The resulting glasses showed an amorphous structure with  $[\text{BO}_3]$  and  $[\text{BO}_4]$  building blocks varied according to the ratio of substitutive ions. This changes in the microstructure have reflected on the characteristic temperatures of the glasses.

The minimum Tg was assigned to G3, while the highest Tg was determined to G4 of around 625°C. The results indicated that increasing of Pb substitution for Ba has made the glass more thermally unstable. The results have also shown that increasing of Pb in glass enlarges TEC of glass as it weakens the strength of glass network.

The electrical resistivity of glass changed with the concentration of non-bridging oxygen. Glass with low NBOs appeared high electrical resistivity in comparison to the others.

The yield glass is promising to be utilized in advanced applications like joints of glass-metal. It might be utilized in laser assisted sealing as well. This part of the research will be covered in a separate study.

#### REFERENCES

- [1] Bengisu, M. (2016). Borate glasses for scientific and industrial applications: A review. *Journal of Materials Science*, 51: 2199-2242.
- [2] Balasubramanian, P., Büttner, T., Pacheco, V.M., & Boccaccini, A.R. (2018). Boron-containing bioactive glasses in bone and soft tissue engineering. *Journal of the European Ceramic Society*, 38(3): 855-869. <https://doi.org/10.1016/j.jeurceramsoc.2017.11.001>
- [3] Chialanza, M.R., Azcune, G., Pereira, H.B., Faccio, R. (2021). New perspective on thermally stimulated luminescence and crystallization of barium borate oxyfluoride glasses. *Crystals*, 11(7): 745. <https://doi.org/10.3390/cryst11070745>
- [4] Zenhom, K., Ebrahim, N.M., Mohammad, S.S., Saudi, H.A. (2024). Role of  $\text{La}_2\text{O}_3$  in enhancement the properties of the  $\text{BaO-B}_2\text{O}_3$  glass system: Optical and radiation shielding study. *Optical and Quantum Electronics*, 56(2): 167. <https://doi.org/10.1007/s11082-023-05692-x>
- [5] Kamil, S.M., Abul-Magd, A.A., El-Gammal, W., Saudi, H.A. (2022). Impact of the structural changes on the attenuation properties of some nickel borate-based glasses containing lead and lanthanum cations for gamma-ray shielding applications. *Journal of Radiation and Nuclear Applications*, 7(1): 21-26. <https://doi.org/10.18576/jrna/010103>
- [6] Manyum, P., Rittisut, W., Wantana, Ruangtaweeep, Y., Rujirawat, S., Kamonsuangkasem, K., Yimnirun, R., Prasatkhetragarn, A., Intachai, N., Kothan, S., Kim, H.J., Kaewkhao, J. (2023). Structural and luminescence properties of transparent borate glass co-doped with  $\text{Gd}_3^+/\text{Pr}_3^+$  for photonics application. *Materials Today Communications*, 37: 107078. <https://doi.org/10.1016/j.mtcomm.2023.107078>
- [7] Winchell, A. N. (1932). The microscopic characters of artificial inorganic solid substances or artificial minerals. *Soil Science*, 33(6): 492.
- [8] Bakal, A., Mat, M.D. (2017). A novel two-layered glass-ceramic sealant design for solid oxide fuel cells. *International Journal of Energy Research*, 41(5): 628-636. <https://doi.org/10.1002/er.3639>
- [9] Riskin, D.K., Bertram, J.E., Hermanson, J.W. (2016). The evolution of terrestrial locomotion in bats: The bad, the ugly, and the good. *Understanding Mammalian Locomotion: Concepts and Applications*, pp. 307-323. <https://doi.org/10.1002/9781119113713.ch12>
- [10] Hogan, R.E. (1975). A review of solder glasses. *Electrocomponent Science and Technology*, 2: 163-169. <https://doi.org/10.1155/APEC.2.163>
- [11] Wong-Ng, W., Roth, R.S., Vanderah, T.A., McMurdie, H.F. (2001). Phase equilibria and crystallography of ceramic oxides. *Journal of Research of the National Institute of Standards and Technology*, 106(6): 1097. <https://doi.org/10.6028/jres.106.059>
- [12] Donald, I.W., Mallinson, P.M., Metcalfe, B.L., Gerrard, L.A., Fernie, J.A. (2011). Recent developments in the preparation, characterization and applications of glass-and glass-ceramic-to-metal seals and coatings. *Journal of Materials Science*, 46: 1975-2000. <https://doi.org/10.1007/s10853-010-5095-y>
- [13] Elkholly, M.M. (2010). Thermoluminescence of  $\text{B}_2\text{O}_3\text{-Li}_2\text{O}$  glass system doped with MgO. *Journal of Luminescence*, 130(10): 1880-1892. <https://doi.org/10.1016/j.jlumin.2010.05.002>
- [14] Tekin, E., Ege, A., Karali, T., Townsend, P.D., Prokić, M. (2010). Thermoluminescence studies of thermally treated  $\text{CaB}_4\text{O}_7$ : Dy. *Radiation Measurements*, 45(7): 764-767. <https://doi.org/10.1016/j.radmeas.2010.04.009>
- [15] Pimentel, N.B., Mastelaro, V.R., M'peko, J.C., Martin, S.W., Rojas, S.S., De Souza, J.E. (2018). Structural and electrical characterization of glasses in the  $\text{Li}_2\text{O-CaO-B}_2\text{O}_3$  system. *Journal of Non-Crystalline Solids*, 499: 272-277. <https://doi.org/10.1016/j.jnoncrysol.2018.07.024>
- [16] Isokawa, Y., Hirano, S., Kawano, N., Okada, G., Kawaguchi, N., Yanagida, T. (2018). Dosimetric and scintillation properties of Ce-doped  $\text{Li}_3\text{PO}_4\text{-B}_2\text{O}_3$  glasses. *Journal of Non-Crystalline Solids*, 487: 1-6. <https://doi.org/10.1016/j.jnoncrysol.2018.02.015>
- [17] Rodriguez Chialanza, M., Castiglioni, J., Fornaro, L. (2012). Crystallization as a way for inducing

- thermoluminescence in a lead borate glass. *Journal of Materials Science*, 47: 2339-2344. <https://doi.org/10.1007/s10853-011-6050-2>
- [18] Bäck, L.G., Ali, S., Karlsson, S., Möncke, D., Kamitsos, E.I., Jonson, B. (2019). Mixed alkali/alkaline earth-silicate glasses: Physical properties and structure by vibrational spectroscopy. *International Journal of Applied Glass Science*, 10(3): 349-362. <https://doi.org/10.1111/ijag.13101>
- [19] Kashif, I., Ratep, A. (2021). ICMMS-2: Influences the addition of neodymium oxide on structural and optical properties of oxyfluoride lead borate glass. *Egyptian Journal of Chemistry*, 64(3): 1141-1147. <https://doi.org/10.21608/ejchem.2021.55860.3183>
- [20] Selçuk, A., Atkinson, A. (2015). Measurement of Mechanical Strength of Glass-to-Metal Joints. *Fuel Cells*, 15(4), 595-603. <https://doi.org/10.1002/fuce.201500028>
- [21] Levin, E.M., McMurdie, H.F. (1949). The system BaO-B<sub>2</sub>O<sub>3</sub>. *Journal of the American Ceramic Society*, 32(3): 99-105. <https://doi.org/10.1111/j.1151-2916.1949.tb18932.x>
- [22] Emami, S., Martins, J., Andrade, L., Mendes, J., Mendes, A. (2017). Low temperature hermetic laser-assisted glass frit encapsulation of soda-lime glass substrates. *Optics and Lasers in Engineering*, 96: 107-116. <https://doi.org/10.1016/j.optlaseng.2017.04.006>
- [23] Wang, Z., Hu, Y., Lu, H., Yu, F. (2008). Dielectric properties and crystalline characteristics of borosilicate glasses. *Journal of Non-Crystalline Solids*, 354(12-13): 1128-1132. <https://doi.org/10.1016/j.jnoncrysol.2007.01.099>
- [24] Hannora, A.E. (2015). Synthesis of lead-borate glasses using high energy ball milling (attritor). *Journal of Non-Crystalline Solids*, 429: 1-4. <https://doi.org/10.1016/j.jnoncrysol.2015.08.024>
- [25] Szreder, N.A., Barczyński, R.J., Karczewski, J., Gazda, M. (2014). Electrical properties and structure of lead-borate glass containing iron ions. *Solid State Ionics*, 262: 837-840. <https://doi.org/10.1016/j.ssi.2014.01.042>
- [26] Kumar, V., Pandey, O.P., Singh, K. (2010). Structural and optical properties of barium borosilicate glasses. *Physica B: Condensed Matter*, 405(1): 204-207. <https://doi.org/10.1016/j.physb.2009.08.055>
- [27] Pisarski, W.A., Goryczka, T., Wodecka-Duś, B., Płońska, M., Pisarska, J. (2005). Structure and properties of rare earth-doped lead borate glasses. *Materials Science and Engineering: B*, 122(2): 94-99. <https://doi.org/10.1016/j.mseb.2005.05.002>
- [28] Yiannopoulos, Y.D., Chryssikos, G.D., Kamitsos, E.I. (2001). Structure and properties of alkaline earth borate glasses. *Physics and Chemistry of Glasses*, 42(3): 164-172.
- [29] Ouis, M.A., Marzouk, M.A. (2020). Comparative optical, FTIR and photoluminescence spectral analysis of copper ions in BaO-B<sub>2</sub>O<sub>3</sub>, SrO-B<sub>2</sub>O<sub>3</sub> or Bi<sub>2</sub>O<sub>3</sub>-B<sub>2</sub>O<sub>3</sub> glasses and impact of gamma irradiation. *Journal of Luminescence*, 223: 117242. <https://doi.org/10.1016/j.jlum.2020.117242>
- [30] Rada, S., Ristoiu, T., Rada, M., Coroiu, I., Maties, V., Culea, E. (2010). Towards modeling gadolinium-lead-borate glasses. *Materials Research Bulletin*, 45(1): 69-73. <https://doi.org/10.1016/j.materresbull.2009.08.021>
- [31] Othman, H.A., Elkholy, H.S., Hager, I.Z. (2016). FTIR of binary lead borate glass: structural investigation. *Journal of Molecular Structure*, 1106: 286-290. <https://doi.org/10.1016/j.molstruc.2015.10.076>
- [32] Kamitsos, E.I., Patsis, A.P., Karakassides, M.A., Chryssikos, G.D. (1990). Infrared reflectance spectra of lithium borate glasses. *Journal of Non-Crystalline Solids*, 126(1-2): 52-67. [https://doi.org/10.1016/0022-3093\(90\)91023-K](https://doi.org/10.1016/0022-3093(90)91023-K)
- [33] Lin, S.L., Hwang, C.S. (1996). Structures of CeO<sub>2</sub>-Al<sub>2</sub>O<sub>3</sub>-SiO<sub>2</sub> glasses. *Journal of Non-Crystalline Solids*, 202(1-2): 61-67. [https://doi.org/10.1016/0022-3093\(96\)00138-X](https://doi.org/10.1016/0022-3093(96)00138-X)
- [34] Doweidar, H., El-Damrawi, G., El Agammy, E.F. (2014). Structural correlations in BaO-PbO-B<sub>2</sub>O<sub>3</sub> glasses as inferred from FTIR spectra. *Vibrational Spectroscopy*, 73: 90-96. <https://doi.org/10.1016/j.vibspec.2014.05.003>
- [35] Othman, H.A., Herrmann, A., Möncke, D. (2019). Mixed barium-lead borate glasses studied by optical and vibrational spectroscopy. *International Journal of Applied Glass Science*, 10(3): 339-348. <https://doi.org/10.1111/ijag.13100>
- [36] The Photographic Periodic Table of the Elements. (2017). <https://periodictable.com/Properties/A/AtomicRadius.an.pr.html>.
- [37] Hmood, F., Schmidt, F., Goerke, O., Günster, J. (2019). Investigation of chemically modified ICIE16 bioactive glass, Part II. *Journal of Ceramic Science and Technology*, 11(1): 1-9. <https://doi.org/10.4416/JCST2019-00031>
- [38] Höland, W., Beall, G.H. (2013). Handbook of Advanced Ceramics: Chapter 5.1. Glass-Ceramics. Academic Press, pp. 371-38. <https://doi.org/10.1016/B978-0-12-385469-8.00021-6>
- [39] Pablos-martín, A., Rodríguez-López, S., Pascual, M.J. (2020). Processing technologies for sealing glasses and glass-ceramics. *International Journal of Applied Glass Science*, pp. 1-17. <https://doi.org/10.1111/ijag.15107>
- [40] Varshneya, A.K. (2010). Chemical strengthening of glass: Lessons learned and yet to be learned. *International Journal of Applied Glass Science*, 1(2): 131-142. <https://doi.org/10.1111/j.2041-1294.2010.00010.x>
- [41] Bobkova N.M. (2003). Thermal expansion of binary borate glasses and their structure. *Glass Physics and Chemistry*, 29(5): 501-507. <https://doi.org/10.1023/A:1026351416382>
- [42] Bhemarajam J., Prasad, S.P., Babu M.M., Özcan M., Prasad, M. (2021). Investigations on structural and optical properties of various modifier oxides (MO = ZnO, CdO, BaO, and PbO) containing bismuth borate lithium glasses. *Journal of Composites Science*, 5(12): 308. <https://doi.org/10.3390/jcs5120308>
- [43] Petrescu, S., Malkla, M., Constantinescu, M., Anghel, E., Atkinson, I., State, R., Zaharescu, M. (2012). Vitreous and glass-ceramics materials in the SiO<sub>2</sub>-Al<sub>2</sub>O<sub>3</sub>-MeO-M<sub>2</sub>O type system. *Journal of Optoelectronics and Advanced Materials*, 14(7-80): 603-612.
- [44] Monteiro, R.C., Lopes, A.A., Lima, M.M., Veiga, J.P., Silva, R.J., Dias, C.J., Fernandes, M.H. (2012). Sintering, crystallization, and dielectric behavior of barium zinc borosilicate glasses-effect of barium oxide substitution for zinc oxide. *Journal of the American Ceramic Society*, 95(10): 3144-3150. <https://doi.org/10.1111/j.1551-2916.2012.05418.x>